Article

Performance of Cr-doped vanadia/titania catalysts for low-temperature selective catalytic reduction of NO$_x$ with NH$_3$

Rui Yang [a], Haifeng Huang [a,*], Yijie Chen [a], Xixiong Zhang [a], Hanfeng Lu [b,#]

[a] *College of Biological and Environmental Engineering, Zhejiang University of Technology, Hangzhou 310014, Zhejiang, China*
[b] *Institute of Catalytic Reaction Engineering, College of Chemical Engineering, Zhejiang University of Technology, Hangzhou 310014, Zhejiang, China*

ARTICLE INFO

ABSTRACT

Cr–V/TiO$_2$ catalysts with different Cr/V molar ratios for low-temperature selective catalytic reduction (SCR) of NO with NH$_3$ were prepared by impregnation. The samples were characterized using X-ray diffraction, NH$_3$ temperature-programmed desorption, H$_2$ temperature-programmed reduction, and X-ray photoelectron spectroscopy. The results show that doping with Cr ions increased the amounts of weak and medium acid sites on the catalyst surface, as well as the low-temperature reductive capacity for high-valence V ions, and promoted the chemical adsorption of oxygen on the catalyst surface, which enhanced the rate of the SCR reaction. The catalyst with a Cr/V molar ratio of 0.2:0.8 and 10 wt% loading gave the largest amount of weak acid sites and the best NO$_x$-removing performance, with a NO$_x$ conversion greater than 90% at 160–300 °C. This catalyst had high stability in the presence of 0.01% SO$_2$.

1. Introduction

Nitrogen oxides (NO$_x$) emitted from thermal power plants and automobile exhaust gases are major air pollutants. The selective catalytic reduction (SCR) of NO$_x$ with NH$_3$ is the most effective technology for NO$_x$ abatement [1–3]. Currently, V$_2$O$_5$–WO$_3$/TiO$_2$ and V$_2$O$_5$–MoO$_3$/TiO$_2$ are the most widely used catalysts, in a narrow temperature window of 300–400 °C [4]. Most SCR systems are installed behind an economizer that allows the flue gas temperature to exceed 300 °C to maintain high catalytic activity. However, the catalyst life is short because it is easily affected by high concentrations of flue dust, SO$_2$, alkali metals, and other factors. In addition, blockage by (NH$_4$)$_2$SO$_4$ byproducts during high-temperature processes is a

problem that needs to be addressed. The preferred technique is to locate the SCR NO$_x$-removing (DeNO$_x$) unit after the desulfurization equipment in coal-fired power plants [5]. In this process, the flue gas temperature can drop to 250 °C below, at which V-based catalysts do not maintain high NO$_x$ conversions [6].

Recent studies suggest that V catalysts have excellent sulfur resistance [7]. Various methods such as use of additives or different supports, e.g., Sb–V$_2$O$_5$/TiO$_2$ [8], V$_2$O$_5$–CeO$_2$/TiO$_2$ [9], V$_2$O$_5$–WO$_3$/Ti–Si [10], V$_2$O$_5$/CeO$_2$–ZrO$_2$ [11], and V$_2$O$_5$/AC [12] catalysts, have been used to further enhance the low-temperature activities of V catalysts at low temperatures and maintain their high sulfur resistance. The low-temperature activities of these catalysts were improved, but the sulfur resistance of V$_2$O$_5$

decreased.

Improvements in V catalyst activities at low temperatures and maintenance of the sulfur resistance of efficient additive-containing catalysts are particularly important. It has been reported that the low-temperature activity of a Cr_2O_3/TiO_2 catalyst was high because more acid sites were present on the surface [13]. Thirupathi et al. [14] obtained 90% NO_x conversion at 180 °C using CrO_x-doped MnO_x/TiO_2; catalyst characterizations showed that surface acidity (Brønsted and Lewis acid sites) had significantly increased. Tong et al. [15] reported that the conversion of NO reached 80.7% at 330 °C for a Cr–Ce/TiO$_2$ catalyst, but dropped from 80.7% to 62.4% after 10 h of sulfur resistance test. Chen et al. [16] prepared Cr–Mn catalysts using the citric acid method; the catalytic activity reached 98.5% at 120 °C but decreased to about 20% after 5 h of sulfur resistance test. Chromium oxide has good low-temperature activity, but its sulfur resistance needs to be improved.

In this study, Cr–V–O/TiO$_2$ catalysts were prepared using Cr and V as the active components and TiO$_2$ as the carrier. The influence of the Cr/V molar ratio and loading was investigated, the catalysts were characterized, and the catalytic mechanism was investigated.

2. Experimental

2.1. Catalyst preparation

Certain amounts of ammonium metavanadate (AR) and chromium nitrate (AR) were dissolved in deionized water. The solution was adequately stirred in a water bath at 60 °C and mixed with TiO$_2$ powders by magnetic stirring for 20 min. Moisture was removed at 60 °C using a rotary vacuum evaporator. The resulting materials were dried at 110 °C overnight and calcined at 450 °C for 3 h. The samples were compressed into tablets and crushed to 20–30 mesh. CrO_x/TiO_2 and VO_x/TiO_2 catalysts were prepared using the same method. The Cr–V/TiO$_2$ catalysts with different Cr/V molar ratios were denoted by Cr_x–V_{1-x}/TiO$_2$ (x = 0.7, 0.5, 0.3, 0.2, 0.1) and $Cr_{0.2}$–$V_{0.8}$/TiO$_2$ catalysts with different weight percentage loadings were denoted by a wt% $Cr_{0.2}$–$V_{0.8}$/TiO$_2$ (a = 5, 10, 20, 50).

2.2. Catalyst characterization

Powder X-ray diffraction (XRD) patterns were obtained using a SCINTAG XTRA diffractometer (Ni-filtered Cu K_α radiation) operated at 40 kV and 50 mA. Intensity data were recorded in the 2θ range from 10° to 80°, with a step size of 0.04°.

X-ray photoelectron spectroscopy (XPS) was performed using an ESCALab 220i-XL electron spectrometer (VG Scientific Company) with 300 W Al K_α radiation. The pressure was maintained at 3×10^{-9} mbar. The C 1s line at 284.6 eV from carbon was used as a reference, and the binding energies were calculated with respect to this line.

H$_2$ temperature-programmed reduction (H$_2$-TPR) and NH$_3$ temperature-programmed desorption (NH$_3$-TPD) were performed using a Micromeritics Auto Chem FINE SORB-3010E

chemisorption analyzer. Prior to H$_2$-TPR analysis, the samples (200 mg) were treated with Ar (30 mL/min at 150 °C for 30 min, cooled to 80 °C, and flushed for 10 min). The atmosphere was changed to 5% H$_2$/Ar (30 mL/min), and the reactor temperature was increased to 750 °C. For NH$_3$-TPD, the samples (150 mg) were heated in a pure He flow at 400 °C for 1 h, and cooled to 100 °C in a He atmosphere. The samples were treated with anhydrous NH$_3$ for 1 h and then purged with He for 1 h. The temperature was increased linearly at a rate of 10 °C/min, and TPD was performed in pure He over the temperature range 100–900 °C.

2.3. Catalytic activity tests

The SCR activity was measured in a fixed-bed quartz reactor containing 0.5 g of catalyst mixed with 0.5 g of quartz sand, with a gas hourly space velocity (GHSV) of 60000 mL/(h·g). The simulated flue gas composition was as follows: φ(NO) = φ(NH$_3$) = 0.05%, φ(O$_2$) = 5%, φ(SO$_2$) = 0.01% (as needed), φ(water) = 10 vol% (as needed), and balance N$_2$. The total flow rate was 500 mL/min. The concentrations of NO, NO$_2$, O$_2$, and SO$_2$ were monitored continuously using a TESTO350-XL gas analyzer. To ensure stability and accuracy of the data, the data were recorded after 20 min when each test condition was changed.

3. Results and discussion

3.1. XRD analysis

The effects of Cr doping on the bulk structures of the catalysts were investigated using XRD. Fig. 1 shows the XRD patterns of the catalysts. It shows that all the peaks in the patterns were attributable to the anatase phase of TiO$_2$. No diffraction peaks attributed to Cr and V species were observed, suggesting that the low-loaded active phase was highly dispersed on the TiO$_2$ support and had an amorphous or microcrystalline structure.
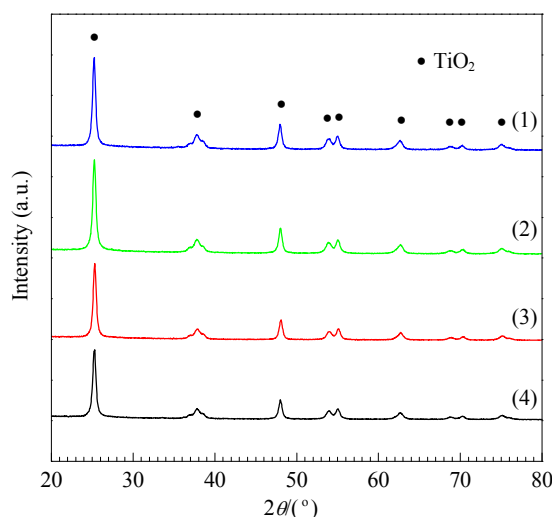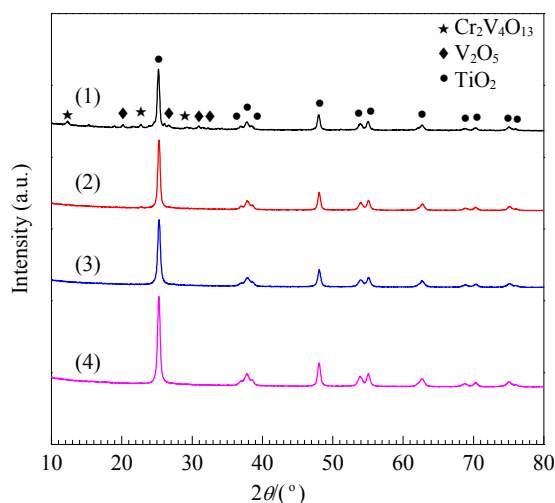

Fig. 1. XRD patterns of catalysts. (1) TiO$_2$; (2) VO$_x$/TiO$_2$; (3) Cr$_{0.2}$–V$_{0.8}$/TiO$_2$; (4) Cr$_x$/TiO$_2$.

Fig. 2. XRD patterns of $Cr_{0.2}–V_{0.8}/TiO_2$ catalysts with different loadings. (1) 50 wt%; (2) 20 wt%; (3) 10 wt%; (4) 5 wt%.

The effect of loading on the catalyst bulk was determined by examining $Cr_{0.2}–V_{0.8}/TiO_2$ catalysts with different loadings. Fig. 2 shows that the composite was highly dispersed on the surface of the TiO_2 support for active component loadings less than 20 wt%. The composite state phase ($Cr_2V_4O_{13}$) was observed on the $Cr_{0.2}–V_{0.8}/TiO_2$ catalyst surface when the loading was 20 wt%. When the loading was increased to 50 wt%, the diffraction peaks of the active component became more apparent.

3.2. NH$_3$-TPD analysis

The surface areas and types of acid sites, determined using NH$_3$-TPD, for catalysts with various Cr/V molar ratios are summarized in Table 1.

NH$_3$-TPD experiments were performed to determine the acid site distributions on the prepared catalysts. The NH$_3$-TPD curves are shown in Fig. 3. The peak centered at about 200 °C is caused by NH$_3$ desorption from weak acid sites, and that centered at about 400 °C is attributed to desorption from medium and strong acid sites. The peak above 400 °C is attributed to NH$_3$ desorption from strong acid sites. Fig. 3 shows that the desorption peak of the VO_x/TiO_2 catalyst in the range 150–350 °C arises from NH$_3$ desorption from weak and medium acid sites distributed on the catalyst surface. Addition of Cr

Table 1
Types of acid sites and surface areas for catalysts with various Cr/V molar ratios determined using NH$_3$-TPD.

Catalyst	Acid site distribution [a]				A_{BET} (m²/g)
	Weak	Medium	Strong	Total	
VO_x/TiO_2	0.10	0.26	—	0.36	56.8
$Cr_{0.1}–V_{0.9}/TiO_2$	0.13	0.34	—	0.47	53.7
$Cr_{0.2}–V_{0.8}/TiO_2$	0.12	0.39	—	0.51	56.2
$Cr_{0.3}–V_{0.7}/TiO_2$	0.13	0.11	0.44	0.68	54.7
$Cr_{0.5}–V_{0.5}/TiO_2$	0.14	0.26	0.52	0.92	52.4
$Cr_{0.7}–V_{0.3}/TiO_2$	0.11	0.30	0.58	1.00	56.2
CrO_x/TiO_2	0.05	0.30	0.59	0.94	83.0

[a] The amount of acidity of $Cr_{0.7}–V_{0.3}/TiO_2$ was assigned as 1.0 and compared with the other samples.
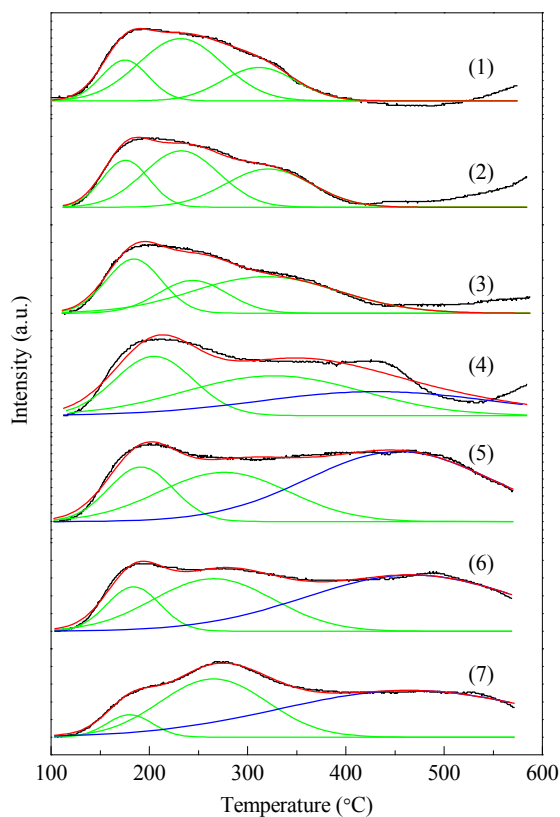
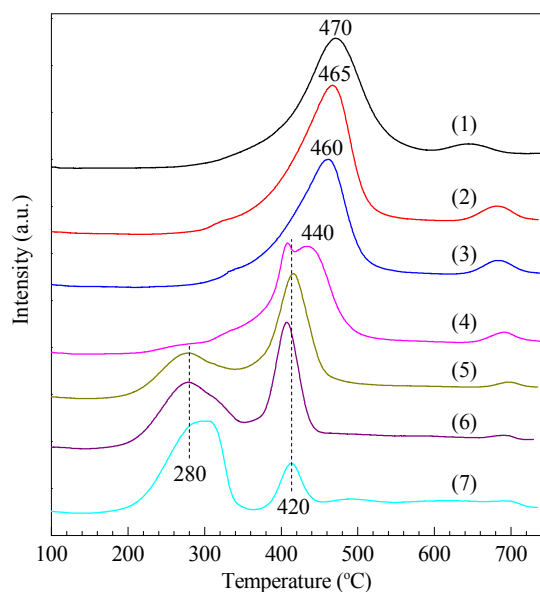**Fig. 3.** NH$_3$-TPD curves for catalysts with various Cr/V molar ratios. (1) VO_x/TiO_2; (2) $Cr_{0.1}–V_{0.9}/TiO_2$; (3) $Cr_{0.2}–V_{0.8}/TiO_2$; (4) $Cr_{0.3}–V_{0.7}/TiO_2$; (5) $Cr_{0.5}–V_{0.5}/TiO_2$; (6) $Cr_{0.7}–V_{0.3}/TiO_2$; (7) CrO_x/TiO_2.

caused broadening of the desorption peak and the amount of chemisorbed NH$_3$ increased. These results suggest that the addition of Cr significantly enhanced the concentration and acidity of acid sites [17]. The desorption peak of the $Cr_{0.2}–V_{0.8}/TiO_2$ catalyst appeared in the range 160–300 °C; this catalyst had the largest amounts of weak and medium acid sites on its surface. When the Cr/V molar ratio was greater than 0.2:0.8, the NH$_3$ desorption peak in the range 450–550 °C was strong. This finding indicates the presence of a large number of strong acid sites on the surfaces of these catalysts; this is not conducive to desorption of NH$_3$ and is unfavorable for SCR activity. The optimum amount of Cr on the V-based catalyst surface would give the highest amount of weak acid sites and the lowest amount of strong acid sites.

3.3. H$_2$-TPR analysis

H$_2$-TPR was used to investigate the catalyst reducibility; the results are shown in Fig. 4. The peak at 470 °C for the VO_x/TiO_2 catalyst can be assigned to the reduction of V^{5+} to V^{3+} [18]. The peak observed above 625 °C is ascribed to unsupported V_2O_5, and could arise from uneven distribution of V on the TiO_2 support. The reduction peak of the catalyst shifted to lower temperatures as the amount of chromium oxide increased. When the Cr/V molar ratio was 0.2:0.8, the reduction temperature of V^{5+} dropped to 460 °C, and no Cr reduction peak was observed. These results indicate good dispersion of Cr species on the cat-

Fig. 4. H$_2$-TPR curves of catalyst with various Cr/V molar ratios. (1) VO$_x$/TiO$_2$; (2) Cr$_{0.1}$–V$_{0.9}$/TiO$_2$; (3) Cr$_{0.2}$–V$_{0.8}$/TiO$_2$; (4) Cr$_{0.3}$–V$_{0.7}$/TiO$_2$; (5) Cr$_{0.5}$–V$_{0.5}$/TiO$_2$; (6) Cr$_{0.7}$–V$_{0.3}$/TiO$_2$; (7) CrO$_x$/TiO$_2$.

alyst surface. A combination of these results with those of the catalyst textural analysis suggests that interactions occurred between the phases (amorphous chromium oxides and vanadium oxides). These interactions could promote the reduction of V^{5+}, which promoted the reaction. When the Cr/V molar ratio was higher than 0.2:0.8, the reduction peak of Cr species was

observed. The CrO$_x$ TPR profile reported in the literature [14] showed two reduction peaks, at 280 and 420 °C; these could be attributed to reduction of Cr^{6+} to Cr^{5+} and of Cr^{5+} to Cr^{3+}, respectively. The results show that the reduction peak of V weakened. Excess Cr therefore occupied the sites of V species, possibly preventing the SCR reaction.

3.4. XPS analysis

XPS was performed to investigate the surface binding energies and valence states of various catalyst species. The results are shown in Table 2 and Fig. 5. As shown in Fig. 5(a), the O 1s photoelectron spectra of the catalysts indicated the presence of two main types of oxygen, namely lattice oxygen (O$_\alpha$), with a binding energy of 529.0–530.0 eV, and surface oxygen (O$_\beta$), with a binding energy of 530.0–531.0 eV [19]. The proportions of surface oxygen in the Cr-doped catalysts were higher than that in the undoped catalyst (Table 2). This finding indicates that the Cr-doped catalyst had a higher proportion of oxygen vacancies than the undoped catalyst. The presence of surface oxygen improves the catalytic activity in the SCR reaction. This effect is an important reason for the increased catalytic activities of the Cr-doped catalysts [20].

The V 2p XPS spectra of the catalyst samples are shown in Fig. 5(b). The peaks at 517.5 and 516.5 eV can be ascribed to the 2$p_{3/2}$ binding energies of V^{5+} and V^{4+} [21]. The surface atomic ratios of V^{4+} to V^{5+} are listed in Table 2; these were obtained by deconvolution. The 10 wt% Cr$_{0.2}$–V$_{0.8}$/TiO$_2$ catalyst had the highest V^{4+}/V^{5+} ratio, and the ratio decreased in the

Table 2
Binding energies and surface atomic concentrations of O, Cr, and V for the prepared catalysts determined from deconvoluted XPS spectra.

Catalyst	Binding energy (eV)			Atomic concentration (%)			V^{4+}/V^{5+}	Cr^{3+}/Cr^{6+}	O$_\beta$/O$_\alpha$
	O 1s	V 2p	Cr 2p	O	Ti (Cr)*	V			
10 wt% VO$_x$/TiO$_2$	530.02, 531.30	516.88, 517.57	—	68.33	25.70	5.97	0.59	—	0.61
5 wt% Cr$_{0.2}$–V$_{0.8}$/TiO$_2$	529.98, 531.17	516.61, 517.26	577.42, 580.05	70.75	26.86	2.39	0.21	0.80	0.92
10 wt% Cr$_{0.2}$–V$_{0.8}$/TiO$_2$	529.80, 530.63	516.88, 517.59	577.31, 579.78	68.06	26.91	5.03	0.73	0.97	1.00
20 wt% Cr$_{0.2}$–V$_{0.8}$/TiO$_2$	529.82, 530.35	516.75, 517.42	576.93, 579.10	70.86	21.97	7.17	0.48	0.88	0.95
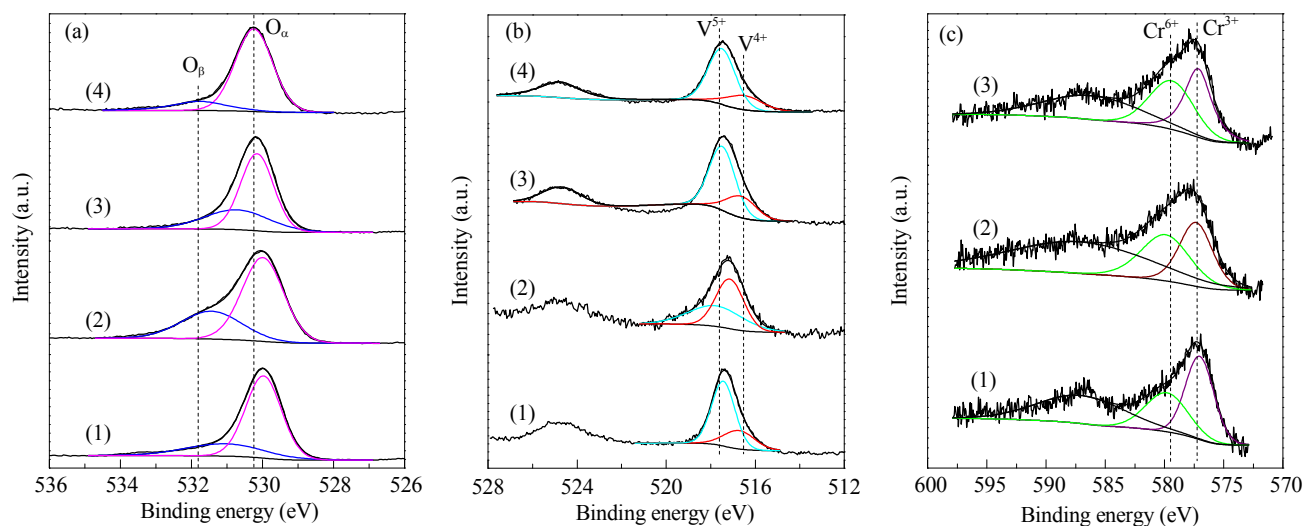
Fig. 5. XPS spectra of O 1s (a), V 2p (b), and Cr 2p (c) of various catalysts. (1) 20 wt% Cr$_{0.2}$–V$_{0.8}$/TiO$_2$; (2) 5 wt% Cr$_{0.2}$–V$_{0.8}$/TiO$_2$; (3) 10 wt% Cr$_{0.2}$–V$_{0.8}$/TiO$_2$; (4) VO$_x$/TiO$_2$.

order 10 wt% $Cr_{0.2}$–$V_{0.8}$/TiO_2 > 10 wt% VO_x/TiO_2 > 20 wt% $Cr_{0.2}$–$V_{0.8}$/TiO_2 > 5 wt% $Cr_{0.2}$–$V_{0.8}$/TiO_2. A large V^{4+}/V^{5+} ratio would generate more free electrons, which are formed from non-stoichiometric V ions in various valence-state-conversion processes.

Fig. 5(c) shows the XPS spectra of Cr 2p on the catalyst surfaces. The Cr atoms on the catalyst surfaces had two valences (Cr^{6+} and Cr^{4+}). The data in Table 2 clearly show that the Cr–V loading on the catalyst had little effect on the Cr^{3+}/Cr^{6+} molar ratio.
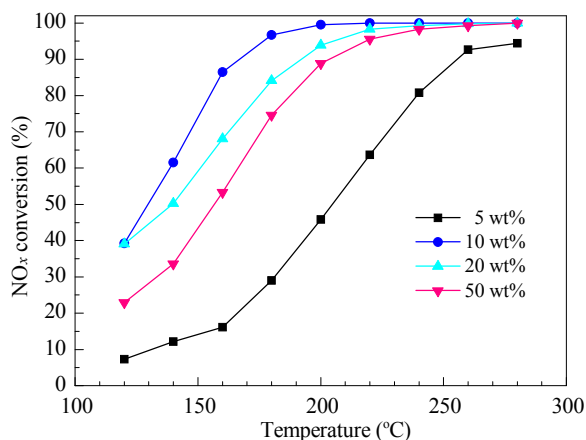
3.5. Catalyst performance

The NO_x conversions over catalysts with various Cr/V molar ratios as a function of reaction temperature are shown in Fig. 6. VO_x/TiO_2 and CrO_x/TiO_2 had poor activities at low temperatures, and CrO_x/TiO_2 had a narrow temperature window. The results show that small variations in the amount of Cr in the Cr–V/TiO_2 catalysts influenced NO_x conversion. The curves for $Cr_{0.1}$–$V_{0.9}$/TiO_2 and $Cr_{0.2}$–$V_{0.8}$/TiO_2 show that the catalytic activities were significantly improved at low temperatures with increasing Cr content because this enhanced the weak acidity of the SCR catalyst. However, excess Cr was unfavorable for the reaction because the active sites on the V-based catalyst were occupied by Cr, as shown by the curves for $Cr_{0.3}$–$V_{0.7}$/TiO_2, $Cr_{0.5}$–$V_{0.5}$/TiO_2, and $Cr_{0.7}$–$V_{0.3}$/TiO_2. The NO_x conversion rate exceeded 90% at 160 °C when the Cr/V molar ratio was 0.2:0.8; this catalytic activity at low temperatures is clearly better than those of the other catalysts, and the temperature window of 160–300 °C was broadened. These findings are in agreement with the NH_3-TPD and H_2-TPR results.

The effects of the catalyst loading on the activities of the $DeNO_x$ catalysts were investigated; the results are shown in Fig. 7. The Cr–V content greatly influenced the NH_3-SCR activity. NO_x conversions over the catalysts decreased in the order 10 wt% > 20 wt% > 50 wt% > 5 wt%. As shown in Table 2, a 5 wt% loading of the $Cr_{0.2}$–$V_{0.8}$/TiO_2 catalyst contained only

Fig. 7. Effect of active phase loading on NO_x conversion. $\varphi(NO) = \varphi(NH_3)$ = 0.05%, $\varphi(O_2)$ = 5%.

2.39% V on the catalyst surface. The number of active sites affects the adsorption rate, therefore the catalyst with a 5 wt% loading decreased the SCR reaction rate. In contrast, the catalyst containing 10 wt% Cr–V had the highest V content on the catalyst surface. Vanadium has a stable oxidation state of +5; V^{4+} is reduced compared with V^{5+} and has one extra electron, which can act as a free electron because there is no constraint on the atom, which shows high mobility and activity. It is therefore reasonable to conclude that an increased V^{4+}/V^{5+} ratio could lead to an increase in the SCR reaction rate, as a result of the free electrons formed in non-stoichiometric V [22]. The catalyst containing 10 wt% Cr–V therefore showed the highest activity and gave nearly 100% NO_x conversion above 200 °C. However, excess loading could lead to aggregation of V_2O_5 and $Cr_2V_4O_{13}$, cover the V active sites, and reduce the $DeNO_x$ catalytic activity.

3.6. Sulfur and water vapor resistance of catalyst

Fig. 8 shows the resistance of the $Cr_{0.2}$–$V_{0.8}$/TiO_2 catalyst to SO_2 poisoning during SCR of NO_x with NH_3. The $Cr_{0.2}$–$V_{0.8}$/TiO_2 catalytic activity was high and NO_x conversion was higher than 75% in the absence of SO_2. In 12 h of test with flue gas contain-

Fig. 6. NO_x conversions over catalysts with various Cr/V molar ratios. Reaction conditions: GHSV = 60000 mL/(h·g), $\varphi(NO) = \varphi(NH_3)$ = 0.05%, $\varphi(O_2)$ = 5%.

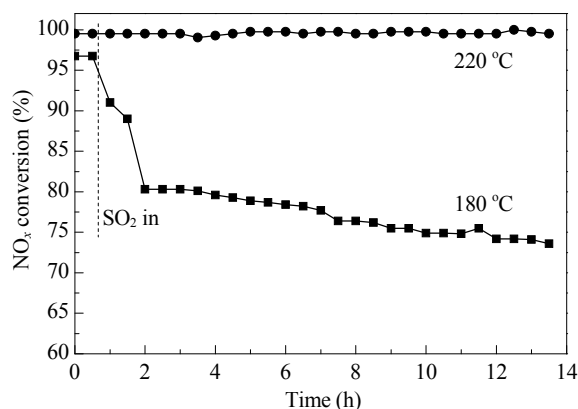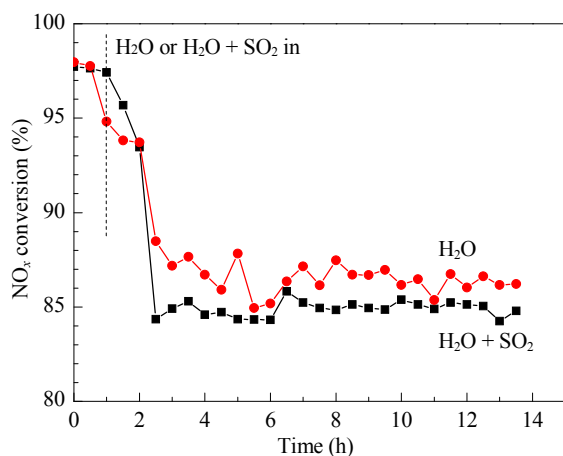**Fig. 8.** Resistance to SO_2 of $Cr_{0.2}$–$V_{0.8}$/TiO_2 catalyst. Reaction conditions: 220 °C or 180 °C, GHSV = 60000 mL/(h·g), [SO_2] = 100 ppm.

Fig. 9. Resistance to water and copresence of water + SO_2 of $Cr_{0.2}$–$V_{0.8}$/TiO_2 catalyst. Reaction conditions: 220 °C, GHSV = 60000 mL/(h·g), $[SO_2]$ = 100 ppm, [water] = 10 vol%.

ing 100 ppm SO_2, the NO_x conversion below 220 °C remained at about 99%. Moreover, no signs of sulfur poisoning were observed. However, the introduction of SO_2 slightly reduced NO_x conversion at 180 °C, because SO_2 on the catalyst surface was easily adsorbed by the V-based catalyst at low temperatures, covering the active sites and ultimately inhibiting the activity.

The influence of water was tested by injecting 10 vol% water into the reaction. As shown in Fig. 9, the presence of water decreased the NO_x conversion by the $Cr_{0.2}$–$V_{0.8}$/TiO_2 catalyst at 220 °C. Several authors have attributed the hindering effect of water vapor to competitive adsorption between water and NH_3 [23]. The $Cr_{0.2}$–$V_{0.8}$/TiO_2 catalyst still had sufficiently high catalytic activity to ensure that NO_x conversion was higher than 85% in the copresence of water and SO_2.

4. Conclusions

Doping of Cr ions increased the amounts of weak and me-

dium acid sites on the VO_x/TiO_2 catalyst surface, promoted the low-temperature reductive capacity of high-valence V ions, and increased the amount of surface oxygen on the catalyst. These factors enhanced the SCR rate. The catalyst with a Cr/V molar ratio of 0.2:0.8 and 10% loading had the largest amount of weak acid sites and gave the best DeNO$_x$ performance, with NO_x conversion greater than 90% at 160–300 °C. This catalyst also showed high stability in the presence of 0.01% SO_2.

References

[1] Martin J A, Yates M, Avila P, Suarez S, Blanco J. *Appl Catal B*, 2007, 70: 330
[2] Yang S J, Wang C Z, Li J H, Yan N Q, Ma L, Chang H Z. *Appl Catal B*, 2011, 110: 71
[3] Yan Z Y, Gao X, Wu J, Jiang Y, Luo Z Y, Ni M J, Cen K F. *J Power Eng*, 2007, 27: 282
[4] Liu C X, Chen L, Li J H, Ma L, Arandiyan H, Du Y, Xu J M, Hao J M. *Environ Sci Technol*, 2012, 46: 6182
[5] Tang X L, Hao J M, Xu W G, Li J H. *Chin J Catal*, 2006, 27: 843
[6] Wu Z B, Jin R B, Liu Y, Wang H Q. *Catal Commun*, 2008, 9: 2217
[7] Yang C, Cheng H, Huang B C. *Chem Ind Eng Prog*, 2014, 33: 907
[8] Maqbool M S, Pullur A K, Ha H P. *Appl Catal B*, 2014, 152-153: 28
[9] Huang Y, Tong Z Q, Wu B, Zhang J F. *J Fuel Chem Technol*, 2008, 36: 616
[10] Huang H F, Zeng L, Lu H F, Zhou C H, Chen Y F. *J Chem Eng Chin Univ*, 2009, 23: 871
[11] Putluru S S R, Riisager A, Fehrmann R. *Catal Lett*, 2009, 133: 370
[12] Zhu Z P, Liu Z Y, Liu S J, Niu H X. *Appl Catal B*, 2001, 30: 267
[13] Pena D A, Uphade B S, Smirniotis P G. *J Catal*, 2004, 221: 421
[14] Thirupathi B, Smirniotis P G. *Appl Catal B*, 2011, 110: 195
[15] Tong H, Luo J, Tong Z Q, Xia B, Luo H. *Environ Eng Sci*, 2011, 28: 711
[16] Chen Z H, Yang Q, Li H, Li X H, Wang L F, Tsang S C. *J Catal*, 2010, 276: 56
[17] Shan W P, Liu F D, He H, Shi X Y, Zhang C B. *Appl Catal B*, 2012, 115-116: 100
[18] Li Q, Yang H S, Nie A M, Fan X Y, Zhang X B. *Catal Lett*, 2011, 141: 1237

Graphical Abstract

Performance of Cr-doped vanadia/titania catalysts for low-temperature selective catalytic reduction of NO_x with NH_3

Rui Yang, Haifeng Huang *, Yijie Chen, Xixiong Zhang, Hanfeng Lu *
Zhejiang University of Technology
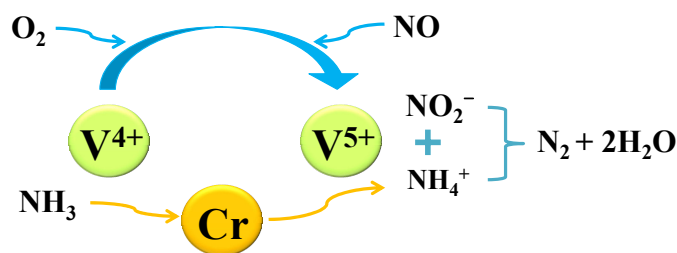
A large V^{4+}/V^{5+} ratio could generate more free electrons, which were formed from the non-stoichiometric vanadium ions at different valence state conversion processes, and they were beneficial in improving the catalytic activity of the SCR reaction.

[19] Nagaveni K, Hegde M S, Ravishankar N, Subbanna G N, Madras G. *Langmuir*, 2004, 20: 2900

[20] Zhao W, Zhong Q, Pan Y X, Zhang R. *Chem Eng J*, 2013, 228: 815

[21] Chang H Z, Li J H, Chen X Y, Ma L, Yang S J, Schwank J W, Hao J M.

Catal Commun, 2012, 27: 54

[22] Choi S H, Cho S P, Lee J Y, Hong S H, Hong S C, Hong S I. *J Mol Catal A*, 2009, 304: 166

[23] Busca G, Lietti L, Ramis G, Berti F. *Appl Catal B*, 1998, 18: 1